3B Containment Hydrodynamic Loads

The information in this appendix of the reference ABWR DCD, including all subsections, tables, and figures, is incorporated by reference with the following departures.

STD DEP T1 2.4-3

STD DEP 3B-1

STD DEP 6.2-2 (Table 3B-1, Figure 3B-13)

STD DEP Admin (Figures ~~3B-11~~, 3B-21, 3B-24, 3B-26)

As required by Section IV.A.3 of the ABWR Design Certification Rule, the plant-specific DCD must physically include the proprietary and safeguards information referenced in the ABWR DCD. Appendix 3B in the reference ABWR DCD references proprietary information.That proprietary information ~~is provided below~~, has finality in accordance with Section VI.B.2 of the ABWR Design Certification Rule, and does not constitute a supplement to or departure from the reference ABWR DCD.

~~ABWR Licensing Topical Report (LTR) NEDO-33372 "ABWR Containment Analysis," dated September 2007, provides a revised containment analysis. The markups provided in the LTR for pages B-2 through B-5 are incorporated by reference.~~

3B.2.2.3 Small Break Accident (SBA)

STD DEP Admin

The SBA is defined as an event in which the fluid loss from the RPV is insufficient to either depressurize the reactor or result in a decrease of reactor water level. Following the break, the drywell pressure will slowly increase until the high drywell pressure scram setting is reached. The reactor will scram, but the MSIVs ~~do not close immediately~~ remain open, and close when reactor water level decreases to RPV Level 1.5.

As a result of a postulated MSIV closure, the SRVs will initially discharge to control reactor vessel pressure in response to the isolation transient. Following the initial SRV discharge, SRV cycling will occur at the SRV setpoint pressure. When the temperature of the suppression pool reaches the Technical Specification limit of ~~54°C~~ 48.9°C *during normal operation, the operator will take action to begin a controlled depressurization of the reactor vessel, using manual operation of the SRVs if the MSIVs are closed, or using the main condenser if the MSIVs are open. The rate of depressurization, and thus the total duration of the SBA event, is dependent on operator action. A conservative value for analysis is taken as 56°C/h.*

3B.3.3 Quencher Condensation Performance

STD DEP Admin

Recent studies, subsequent to the issuance of NUREG-0783, conclude that steady steam flow through quencher devices (like the X-quencher) is expected to be a stable and smooth condensation process over the full range of pool temperature up to saturation. It is also concluded that the condensation loads ~~*for stem discharge*~~ from X-quencher are *less than the loads from equivalent straight pipes.* Figure 3B-8 shows typical pressure amplitudes due to condensation of steam from X-quenchers. *These recent studies are described and discussed in Reference 3B-5.*

3B.4.1 Pressure and Temperature Transients

STD DEP 6.2-2

A LOCA causes a pressure and temperature transient in the drywell and wetwell due to mass and energy released to the drywell. The severity of this transient loading condition depends upon the type and size of LOCA. ~~*Section 6.2 provides pressure and temperature transient data in the drywell and wetwell for the most severe LOCA case [design basis accident (DBA)]. This transient data establish the structural loading conditions in the containment.*~~ Bounding pressure and temperature envelope curves for large, intermediate, and small break LOCAs are used to establish the structural loading conditions in the containment.

3B.4.2.1 Pool Boundary Loads

STD DEP 6.2-2

Structures located between 0 and ~~*7m*~~8.5m *above the initial surface will be subjected to impact load by an intact water ligament, where the* ~~*7m*~~8.5m *value corresponds to the calculated maximum pool swell height. The load calculation methodology will be based on that approved for Mark II and Mark III containments (NUREG-0487 and NUREG-0978).*

Structures located at elevations between the ~~*7m*~~8.5m *and* ~~*10.3m*~~11.7m *will be subjected to froth impact loading. This is based on the assumption that bubble breakthrough (i.e., where the air bubbles penetrate the rising pool surface) occurs at* ~~*7m*~~8.5m *height, and the resulting froth swells to a height of 3.3m.* ~~*This froth swell height is the same as that defined for Mark III containment design and this.*~~This *is considered to be conservative for the ABWR design. Because of substantially smaller wetwell gas space volume (about 1/5th of the Mark III design), the ABWR containment is expected to experience a froth swell height substantially lower than the Mark III design. The wetwell gas space is compressed by the rising liquid slug during pool swell, and the resulting increase in the wetwell gas space pressure will decelerate the liquid slug before the bubble break-through process begins. The load calculation methodology will be based on that approved for the Mark III containment (NUREG-0978).*

*As shown in Figure 3B-13 the gas space above the ~~10.3 m~~*11.7m *elevation will be exposed to spray condition ~~including~~*which is expected to induce *no significant loads on structures in that region.*

*As drywell air flow through the horizontal vent system decreases and the air/water suppression pool mixture experiences gravity-induced phase separation, pool upward movement stops and the "fallback" process starts. During this process, structures between the bottom vent and the ~~10.3m~~*11.7m *elevation can experience loads as the mixture of air and water fall past the structure. The load calculation methodology for ~~the~~defining such loads will be based on that approved for Mark III containment (NUREG-0978).*

3B.4.2.3 Impact and Drag Loads

STD DEP 3B-1

As the pool level rises during pool swell, structures or components located above the initial pool surface (but lower than its maximum elevation) will be subjected to water impact and drag loads. The following equations will be used to compute the applicable impact and drag loads on affected structures.

Impact Load

Flat Target:

$T = (0.011 \times W) / V$ *for* $V \geq 2.13$ *m / s*

$= (0.0016 \times W)$ *for* $V \leq 2.13$ *m / s*

The equation above is replaced with the following equation below:

$T = (0.011 \times W) / V$ for $V \geq 2.13$ m / s

$= (0.0052 \times W)$ for $V < 2.13$ m / s

where

T = Pulse duration, s

D = Diameter of cylindrical pipe, m

W = Width of the flat structure, m

V = Impact velocity, m/s

3B.4.3.2.1 Description of CO Database

STD DEP Admin

A detailed description, evaluation, and discussion of CO data are given in Reference 3B-7.

The test program consisted of a total of 13 simulated blowdowns in sub-scaled test facility representing a one-cell (~~360~~° 36°) sector of the ABWR horizontal vent design, which included a ~~signal~~ single *vertical/horizontal vent module. The subscaled (SS) test*

facility was geometrically (all liner dimensions scaled by a factor of 2.5) similar to the prototypical ABWR design, and the single vertical/horizontal vent module included all three horizontal vents, as shown in Figure 3B-15. In these tests, full-scale thermodynamic conditions were employed. This approach is based on the belief that condensation phenomena at the vent exit are mainly governed by the thermodynamic properties of the liquid and vapor phases. In accordance with this scaling procedure, measured pressure amplitudes are equal to full-scale values at geometrically similar locations, whereas measured frequencies are 2.5 times higher than the corresponding full-scale frequencies.The technical basis for using this scaling approach was based on extensive review and evaluation of the available literature on CO scaling and scaled tests performed for Mark II and Mark III containments, as well as general consensus of technical experts in this field. The CO scaling studies, which have been performed independently by various technical experts, show that for tests in a geometrically scaled facility with full-scale thermodynamic conditions, the measured pressure amplitudes are the same as full-scale values at geometrically similar locations, and measured pressure frequencies are the scale factor times higher than the corresponding full-scale frequencies.

3B.4.3.3.3.3 Loads on Horizontal Vent

STD DEP Admin

For structure evaluation of the horizontal vent pipe and pedestal, an upward load, based on the HVT test data, is conservatively defined as shown in Figure ~~3B-27~~ 3B-33*.*

For building structure response analysis for the evaluation of RPV and its internals, the horizontal vent upward load is specified as shown in Figure ~~3B-28~~ 3B-34*. To bound symmetrical and asymmetrical loading conditions, the following two load cases will be considered and analyzed.*

3B.4.4.1 Exhaust Steam Condensation Loading

STD DEP T1 2.4-3

The RCIC system is a safety system, consisting of a steam turbine, pump, piping, accessories, and necessary instrumentation. ~~The steam turbine exhaust steam piping is ASME Code Class 2 piping, as noted in the RCIC P&ID in Tier 2 Figure 5.4-8.~~

To minimize exhaust steam line vibration and noise levels, the discharge end of the turbine exhaust line will be equipped with a condensing sparger. The sparger design configuration will be similar to that currently used successfully for the operating BWRs. The turbine exhaust piping, including the RCIC sparger, are designed to retain piping pressure integrity and functional capability.

The condensing sparger is expected to produce a very smooth steam condensation operation resulting in low pressure fluctuations in the ~~poll~~ pool*, which would imply low pressure on the pool boundary. ~~During RCIC operation, steam mass flux in the neighborhood of 470.72 PaÞs are expected, which should assure smooth steam condensation process.~~ During the extended RCIC operation, condensing exhaust*

steam will bring the ~~pcll~~ pool *to high temperature. At high ~~pcll~~* pool *temperatures, long plumes consisting of a random two-phase mixture of entrained water and steam bubbles are expected to exist. As reported in Reference 3B-16*, this plume would not shed large coherent bubbles. Large coherent bubbles are a concern because they may drift and collapse in a cooler region of the pool, *~~the condensation of the steam within such a mixture will not give rise to large bubbles that drift in to a cooler region of the pool and suddenly collapse which could transmit~~* potentially producing *significant loads to the pool boundary.*

3B.5 Submerged Structure Loads

STD DEP Admin

During SRV actuations, the dynamic process of the steam blowdown is quite similar to LOCA steam blowdown but the induced load is mitigated by the X-quencher device attached at the end of each discharge ~~device~~ line*. Two types of loads are important. One is due to the water jet formed at the confluence of the X-Quencher ~~arm~~* arms *~~discharges~~ and another is due to the four air bubbles formed between the arms of the X-Quencher. These air bubbles are smaller in size than the LOCA air bubbles, reside longer in the pool, and oscillate as they rise to the free surface of the pool.*

3B.7 References

STD DEP Admin

3B-13 *~~T. H. Chuang, L. C. Chow, and~~ L. E. Lasher, "Analytical Model for Estimating Drag Forces on Rigid Submerged Structures Caused by LOCA and Safety Relief Valve Ramshead Air Discharges"*, Supplement for X-Quencher Air Discharge," *NEDO-21471, Supplement 1~~, June 1978.~~* October 1979.

Table 3B-1 Pool Swell Calculated Values

Description	Value
1. Air bubble pressure (maximum)	~~133.37 kPaG~~190.0kPaG
2. Pool swell velocity (maximum)	6.0 m/s
3. Wetwell airspace pressur (maximum)	~~107.87 kPaG~~155.0kPaG
4. Pool swell height (maximum)	~~7m~~8.5m

[e4]

Table 3B-2 Final ABWR HVT Test Matrix

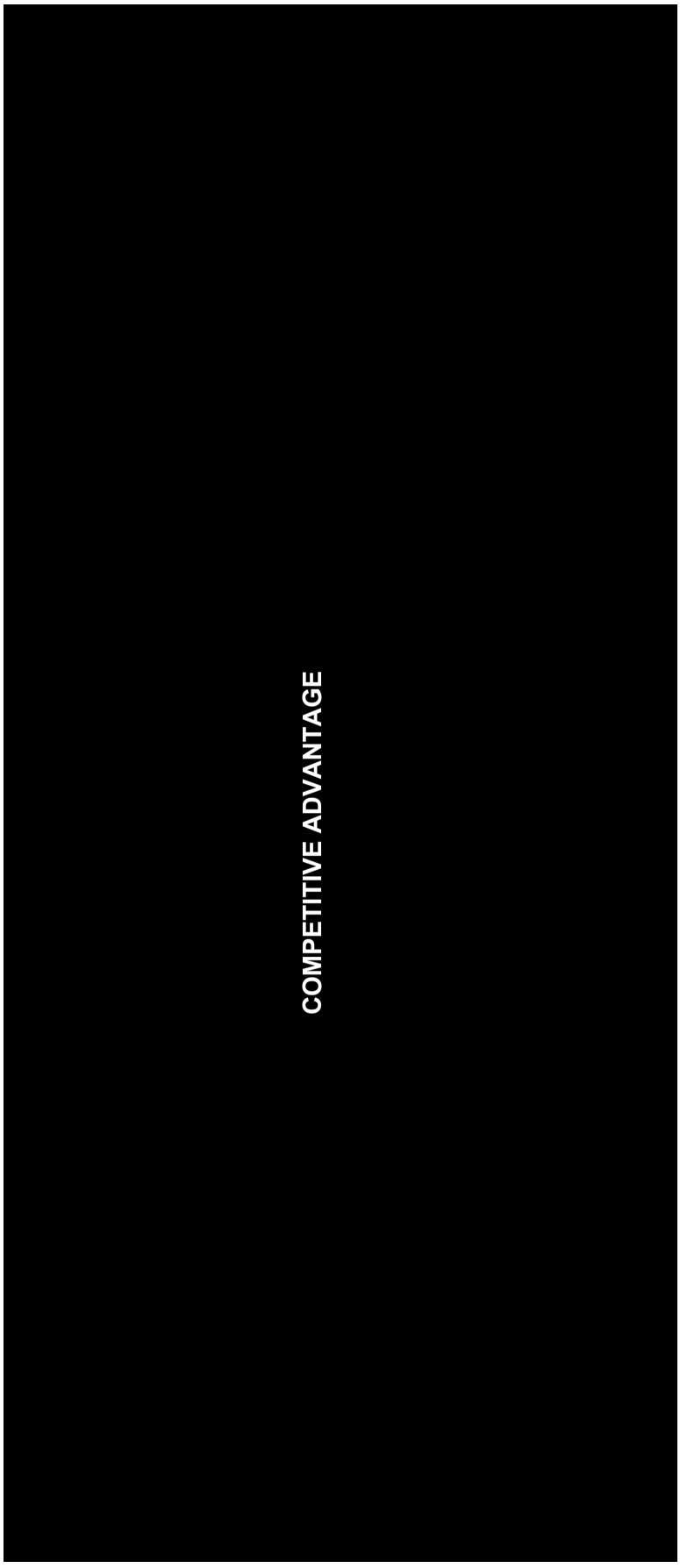

[s4]

[s4]

Table 3B-3 Mean and Standard Deviation of CH POP and PRMS by Test

COMPETITIVE ADVANTAGE

[e4]

[s4]

Table 3B-4 Average Chug Period by 10-Second Segment for Steam Breaks at 21°C (Continued)

COMPETITIVE ADVANTAGE

[e4]

[s4]

Table 3B-5 Average Chug Period by 10-Second Segment for Steam Breaks at 49°C

Table 3B-6 Average Chug Period by 10-Second Segment for Steam Breaks at 68°C

[e4]

[s4]

Table 3B-7 Average Chug Period by 10-Second Segment for Steam Breaks at 21°C, 49°C, and 68°C

Table 3B-8 Pool Swell Model Comparison with PSTF Test Data

[e4]

[s4]

Table 3B-9 Model vs PSTF Test Data Comparison Results Summary at Selected Time

COMPETITIVE ADVANTAGE

[e4]

[s4]

Figure 3B-2 X-Quencher Schematic

[e4]

[s4]

Figure 3B-3 X-Quencher Azimuthal Locations in the ABWR Suppression Pool

[e4]

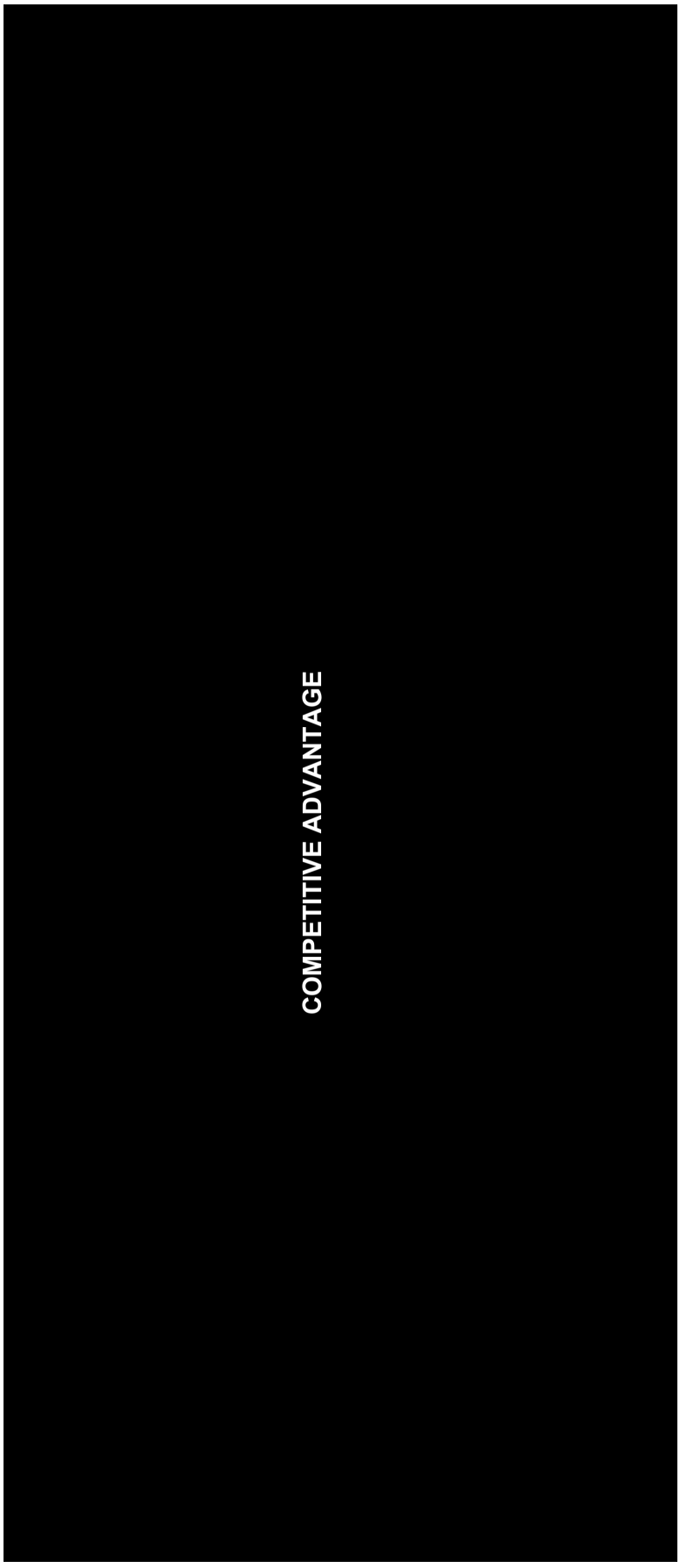

Figure 3B-8 Pool Boundary Pressure Time-History Measured for Second of SRV Condensation

[s4]

[s4]

Figure 3B-9 PSTF Test Data vs PICSM Prediction: Test 5702-11

[e4]

[s4]

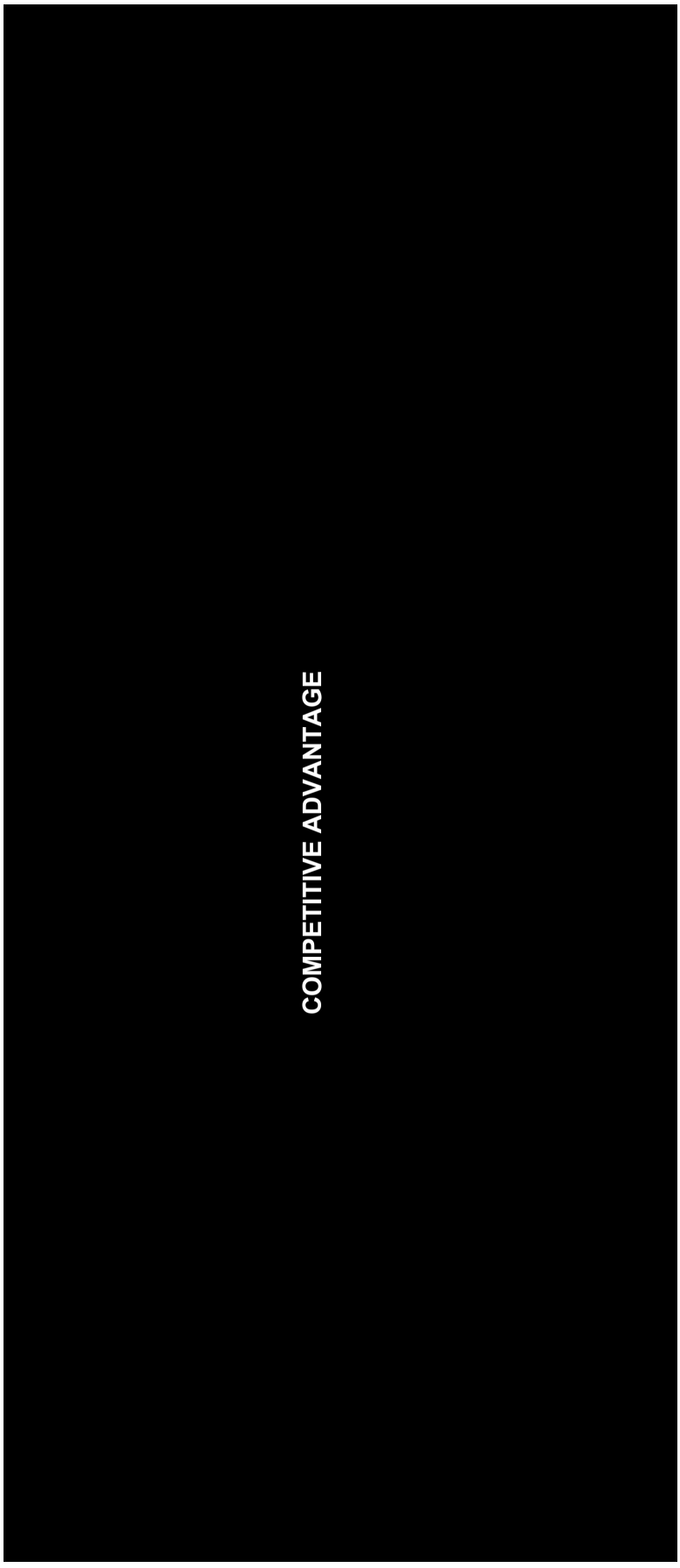

[e4]

Figure 3B-10 PSTF Test Data vs Model Prediction: Test 5806-4

~~Figure 3B-11 Pool Boundary Pressure During Pool Swell, Normalized to Bubble Pressure~~

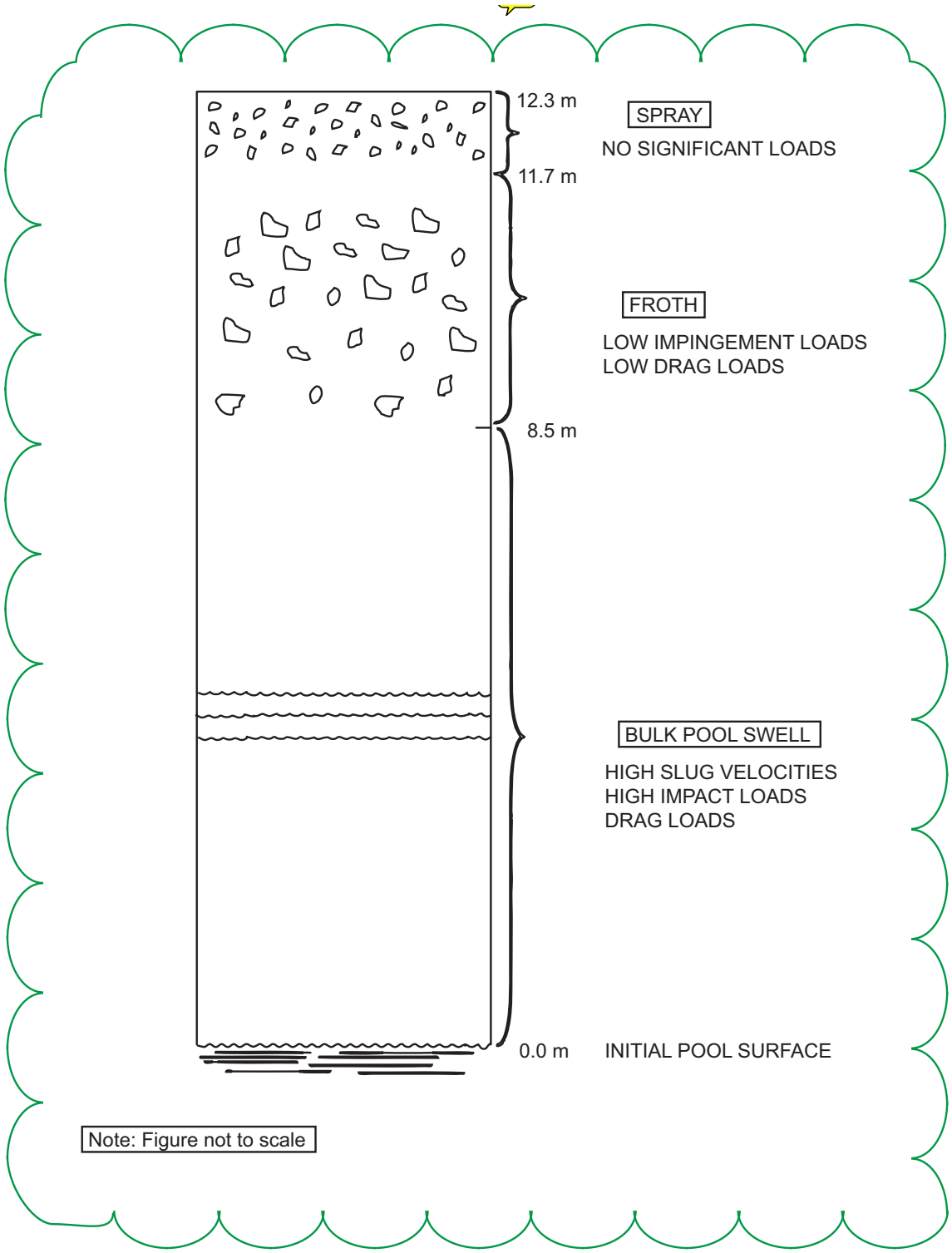

Figure 3B-13 Schematic of the Pool Swell Phenonmenon~~Pool Boundary Pressure During Pool Swell, Normalized to Bubble Pressure~~

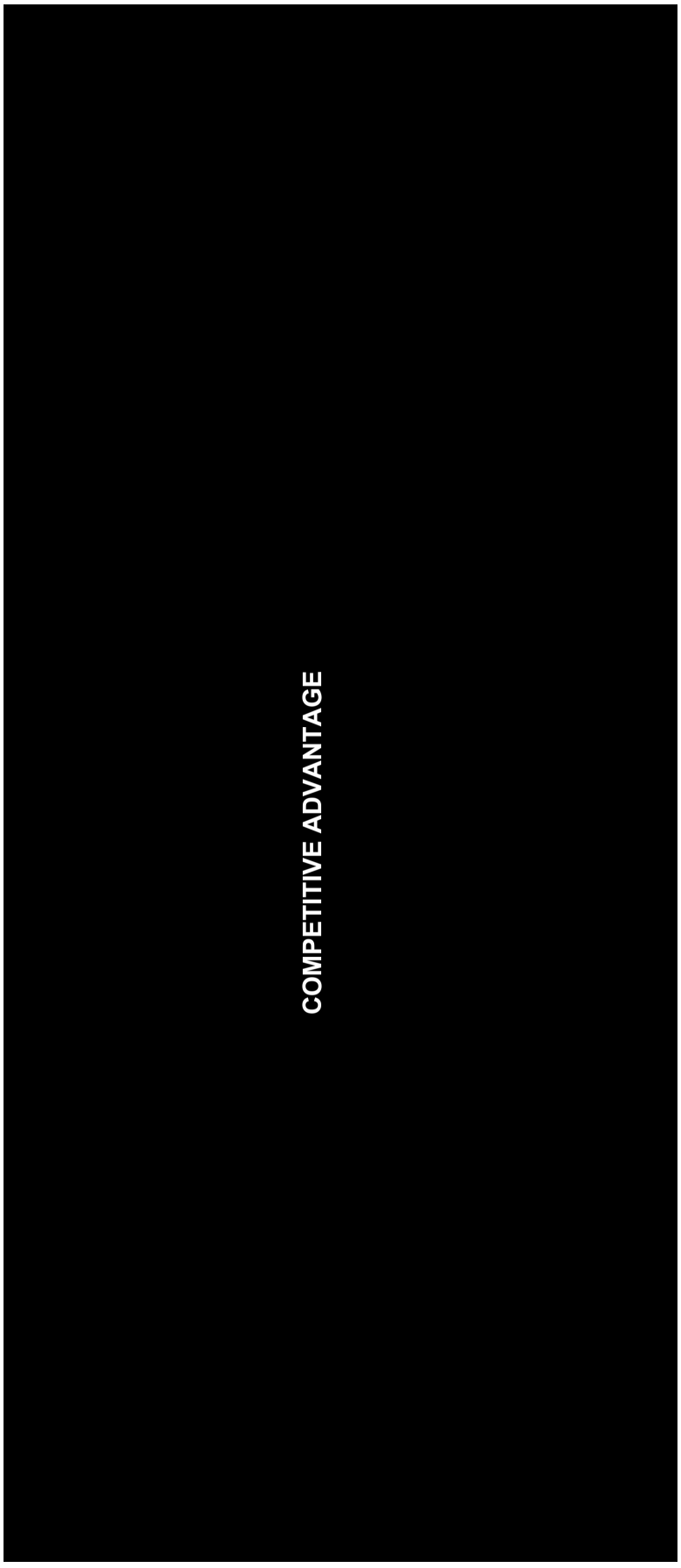

Figure 3B-14 Drag Coefficient for Cylinders Following Impact

[s4]

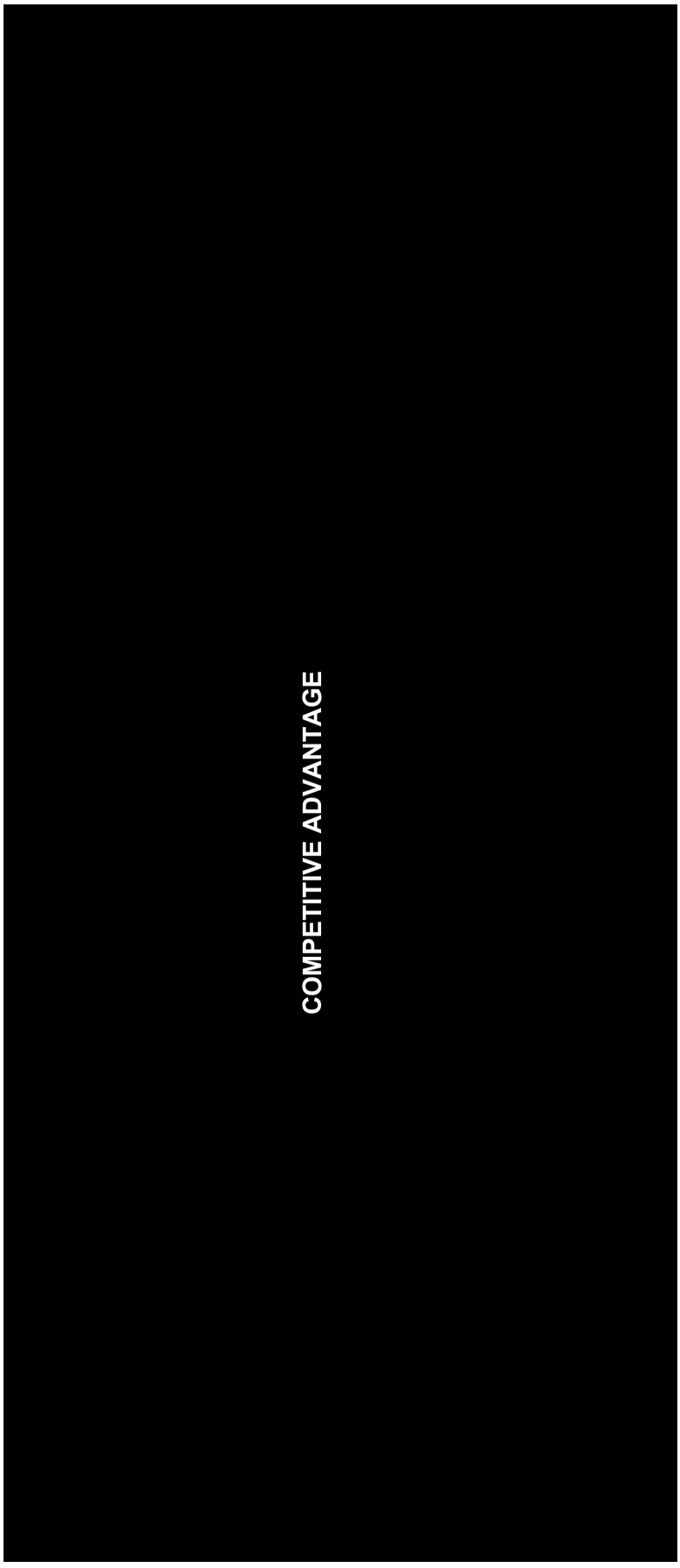

Figure 3B-15 SS Test Facility

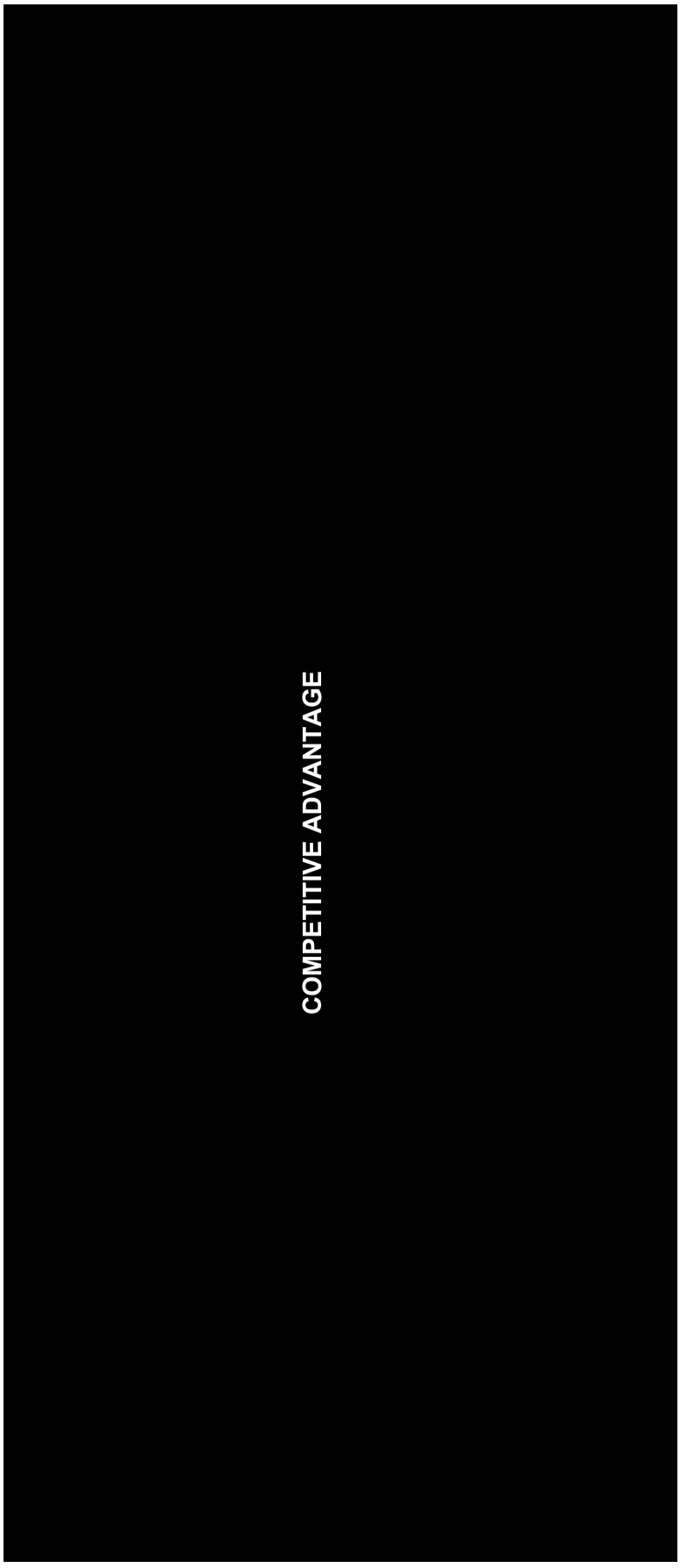

Figure 3B-16 FS Test Facility

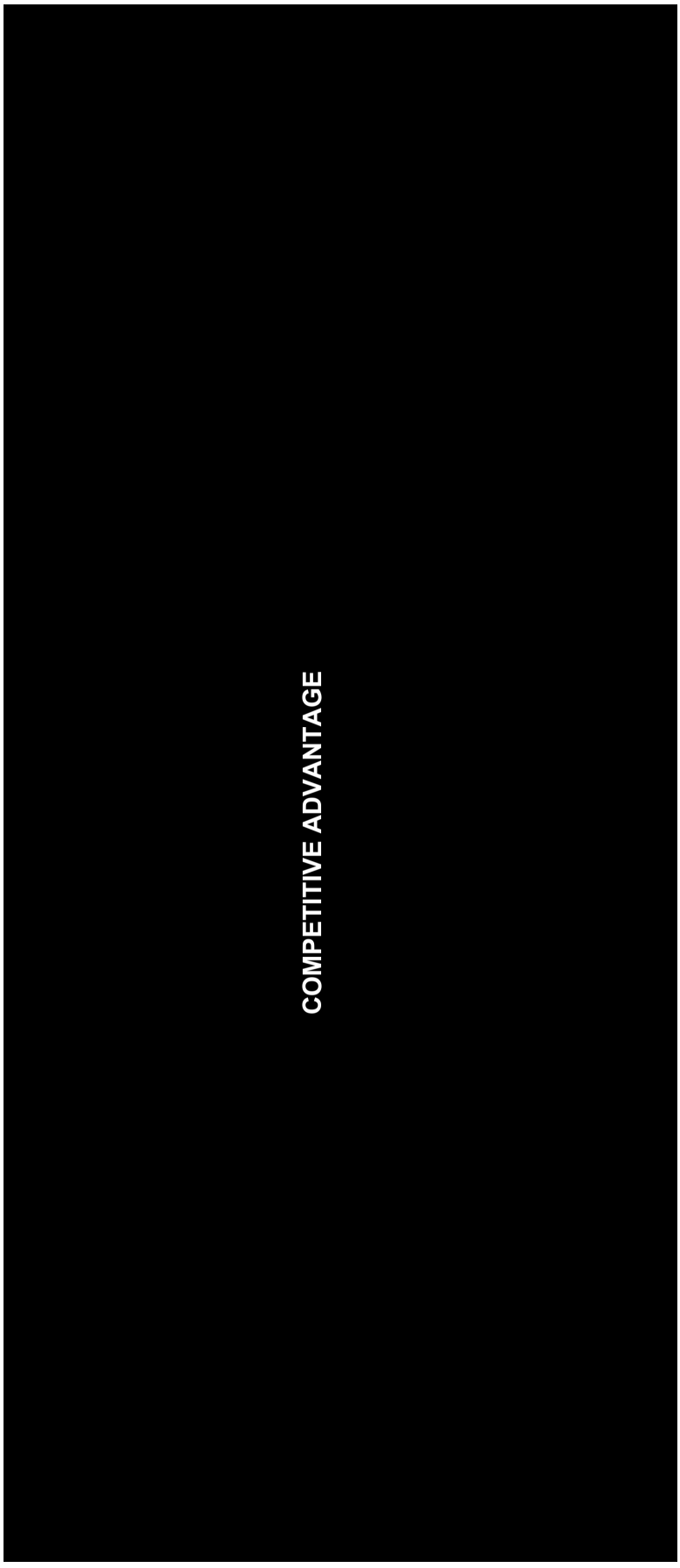

Figure 3B-17 Test Sensors Common to FS* and SS Tests

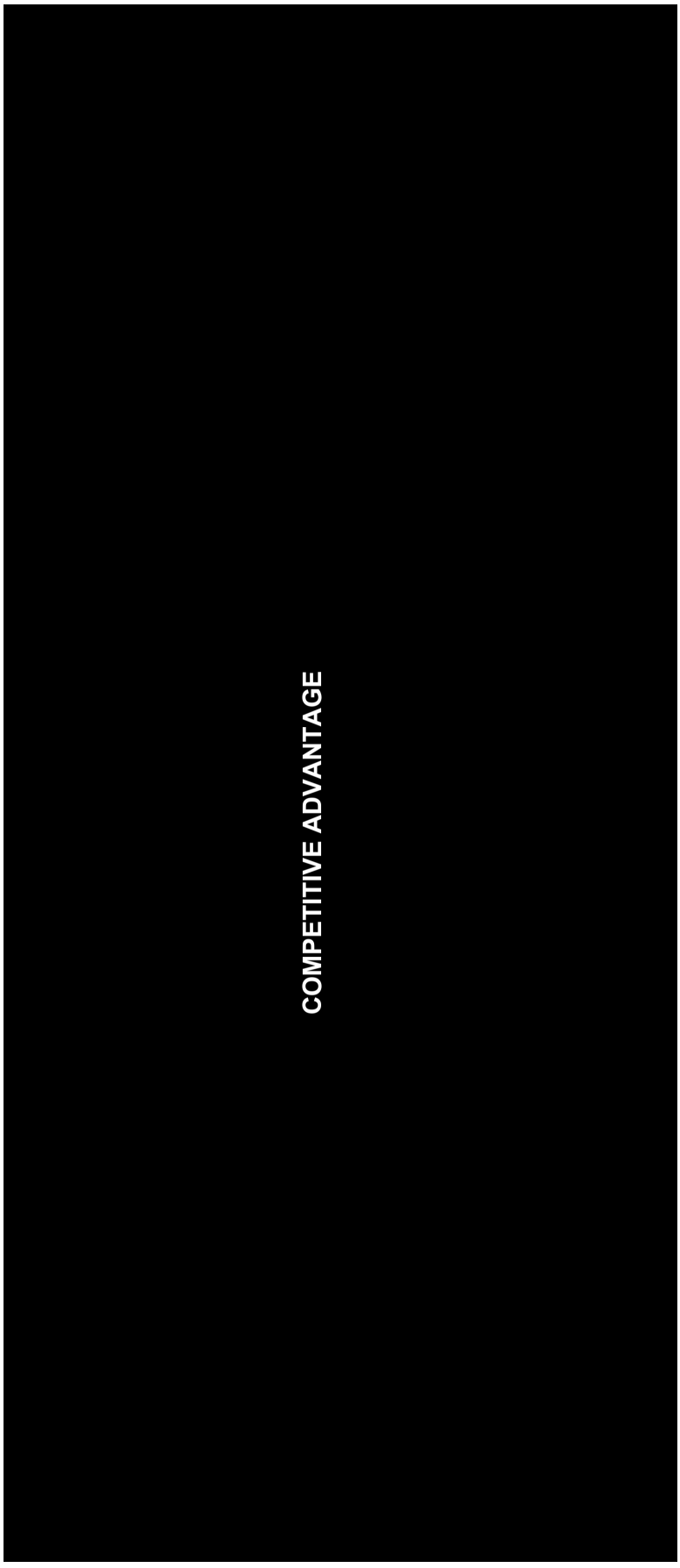

Figure 3B-18 Test Sensors Unique to FS* and SS Tests

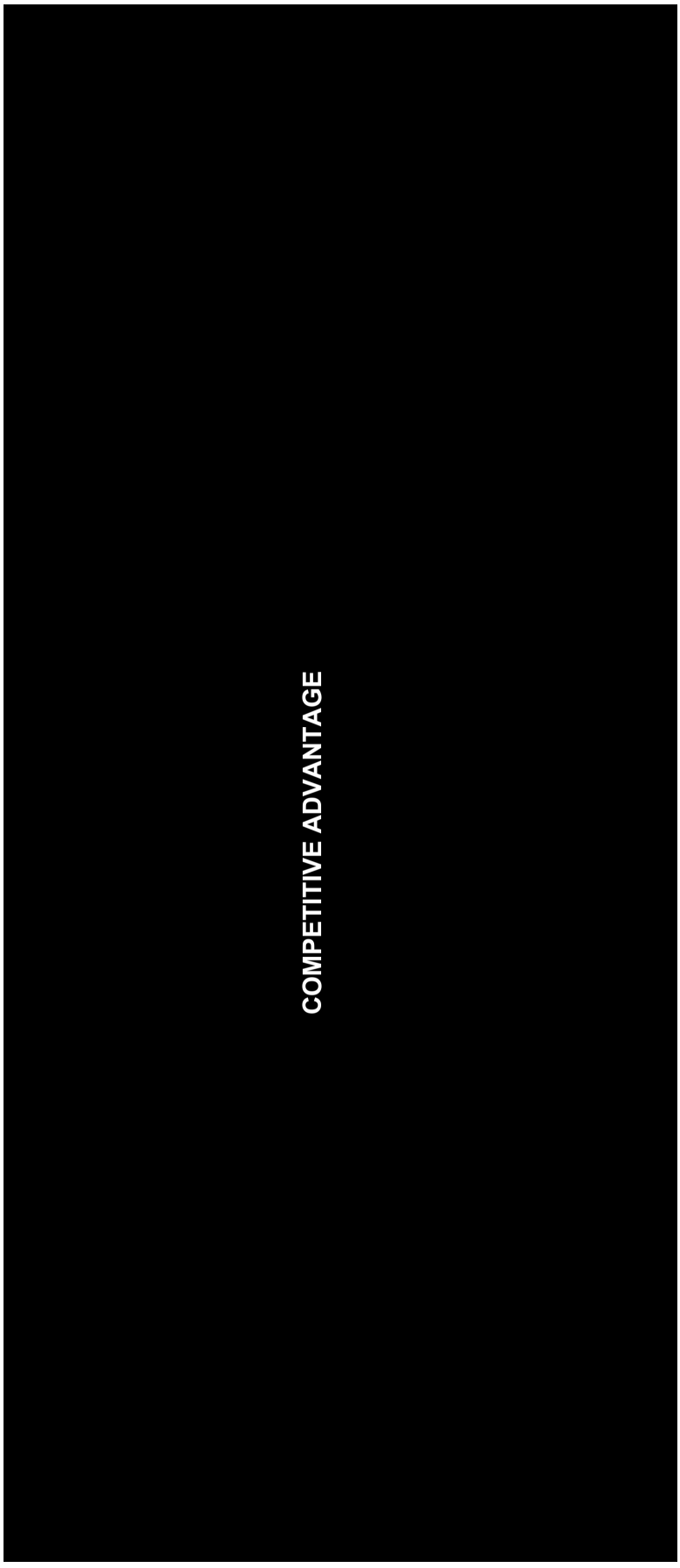

Figure 3B-19 Envelope PSD at 019P for SST-1, 2, 3, 9, 11, and 12

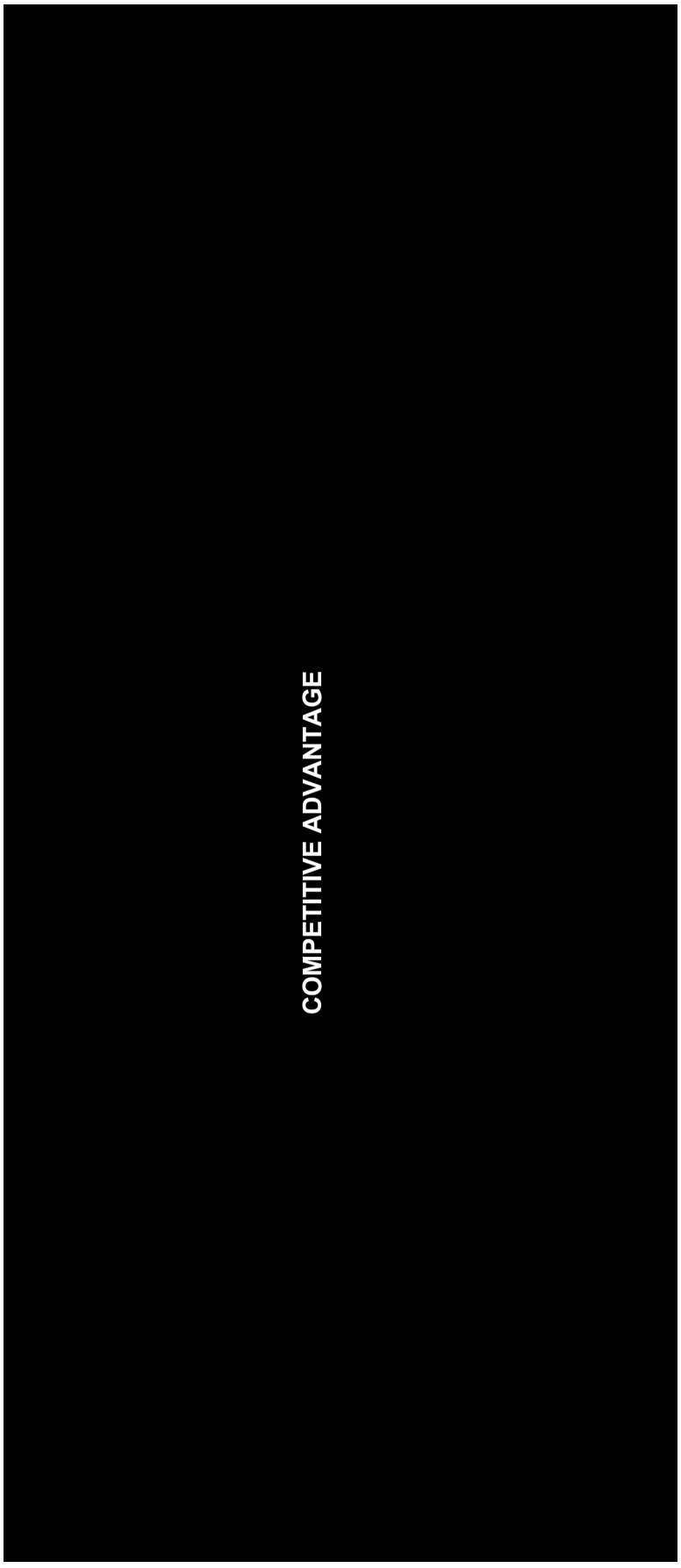

[e4]

Figure 3B-20 Six-Test and Key-Segment Envelope PSDs at 019P

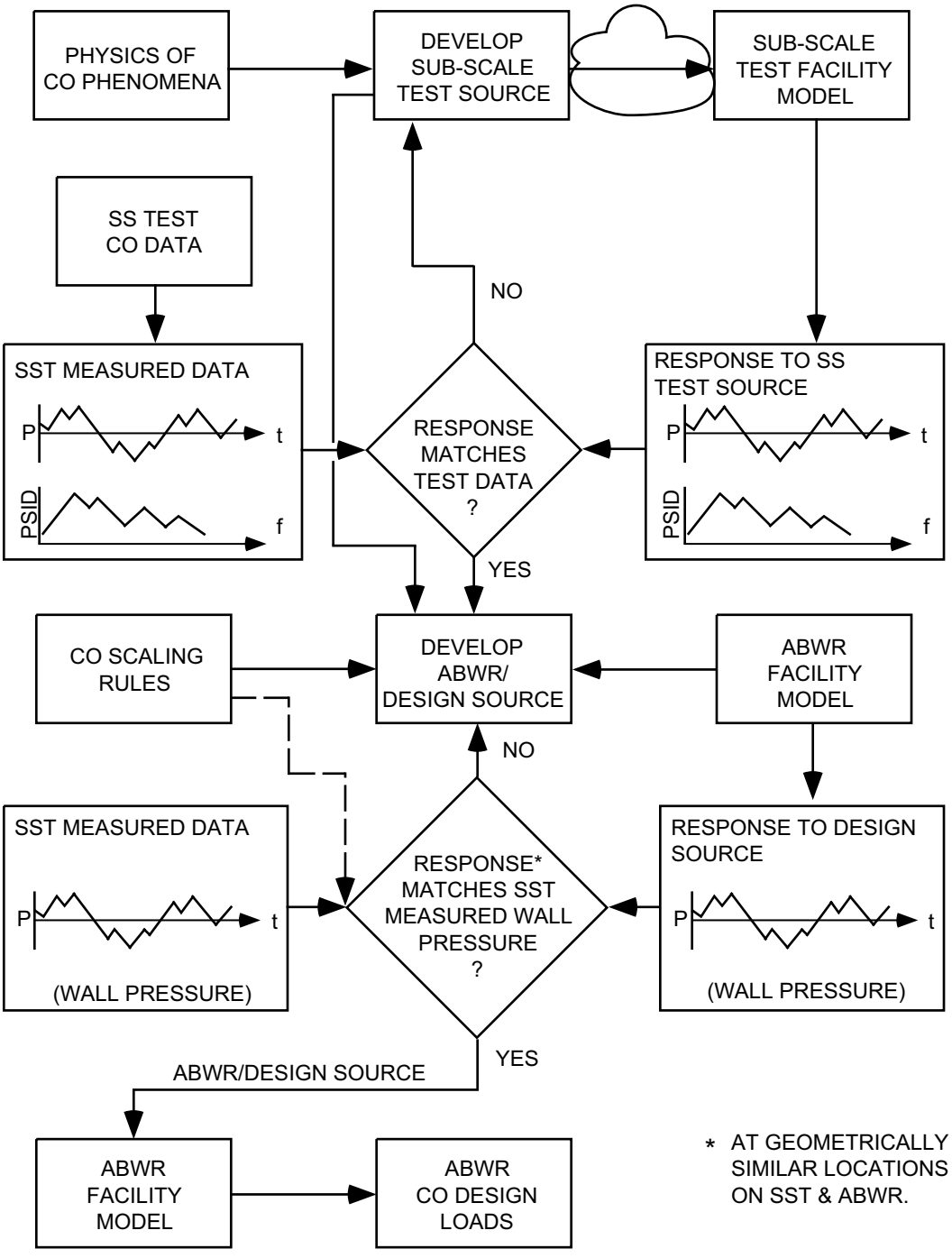

Figure 3B-21 ABWR CO Source Load Methodology

[s4]

COMPETITIVE ADVANTAGE

Figure 3B-22 ABWR Typical Pressure Fluctuation Due to CO

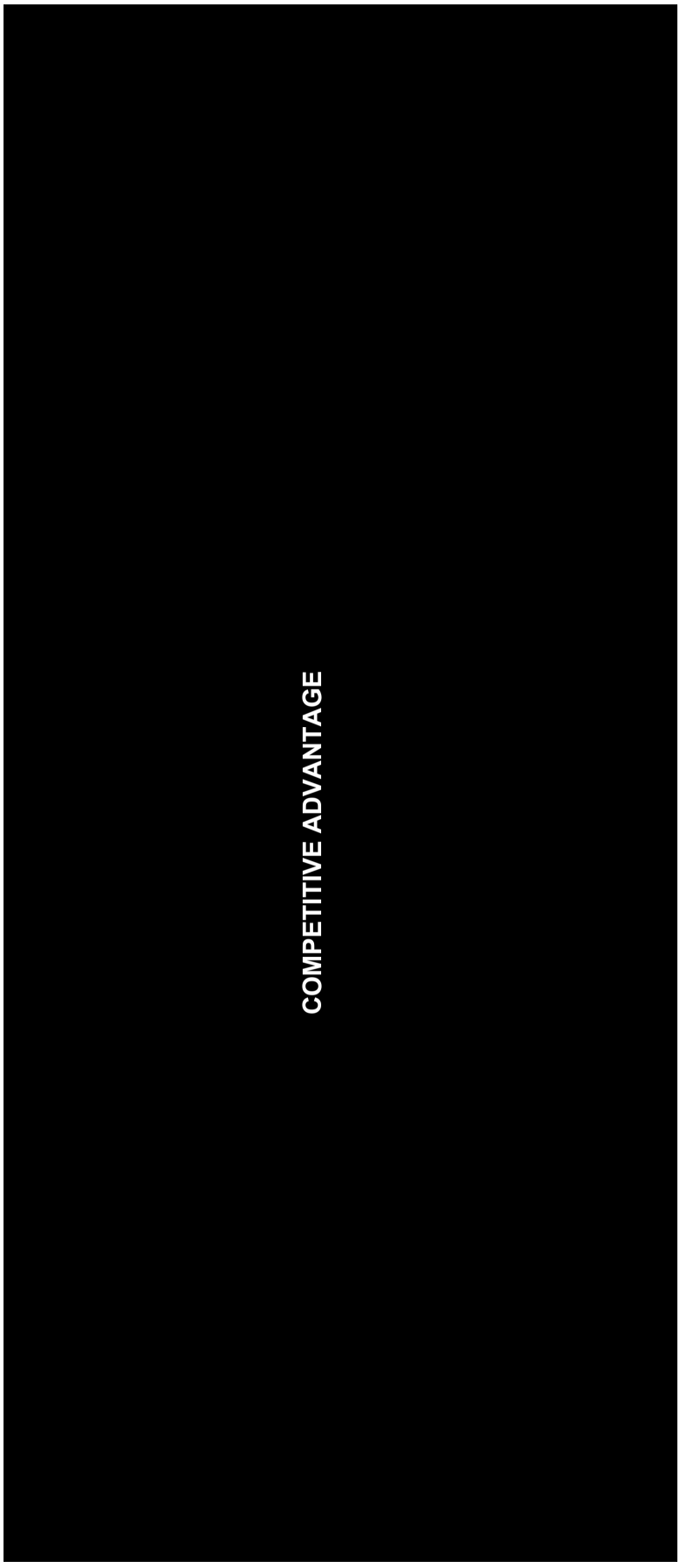

Figure 3B-23 Mark III Typical Pressure Fluctuation Due to CO

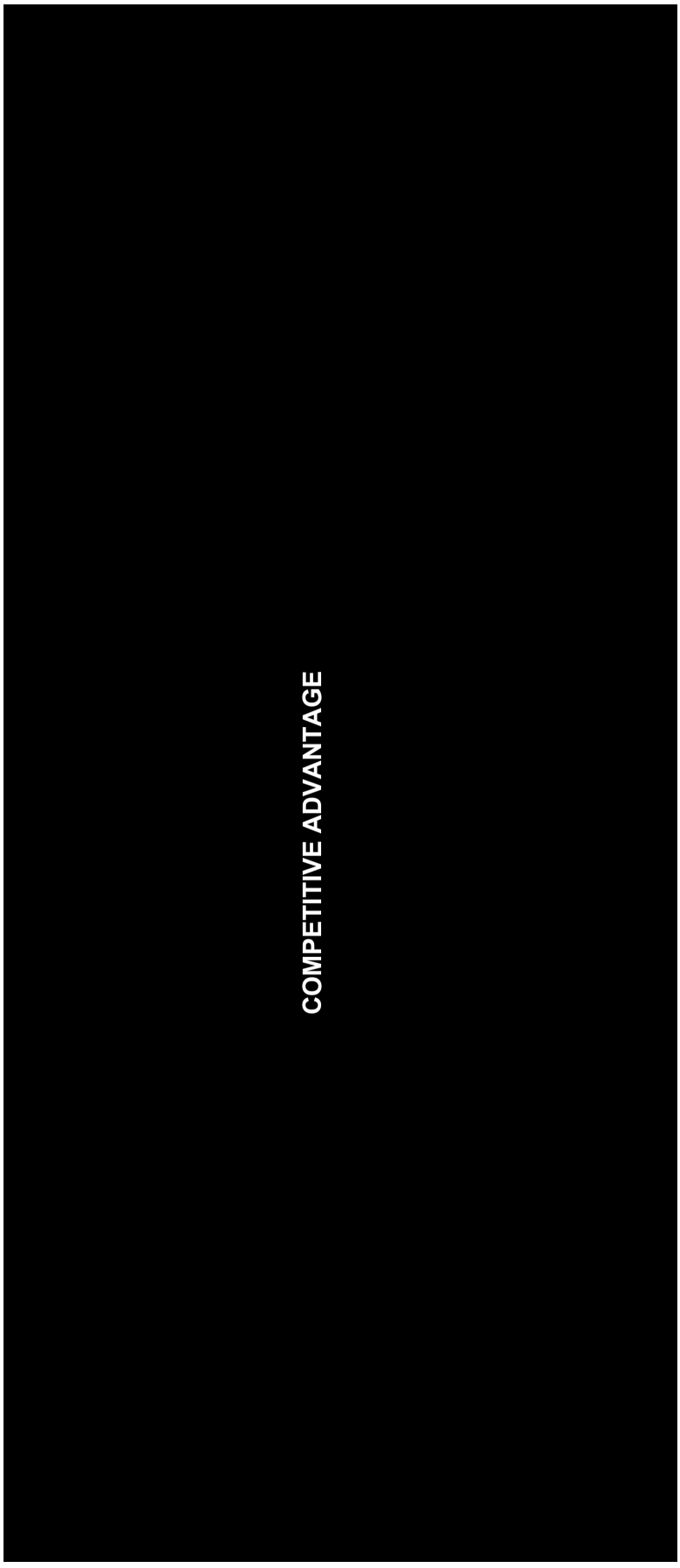

Figure 3B-24 Typical Large Chug (025P)

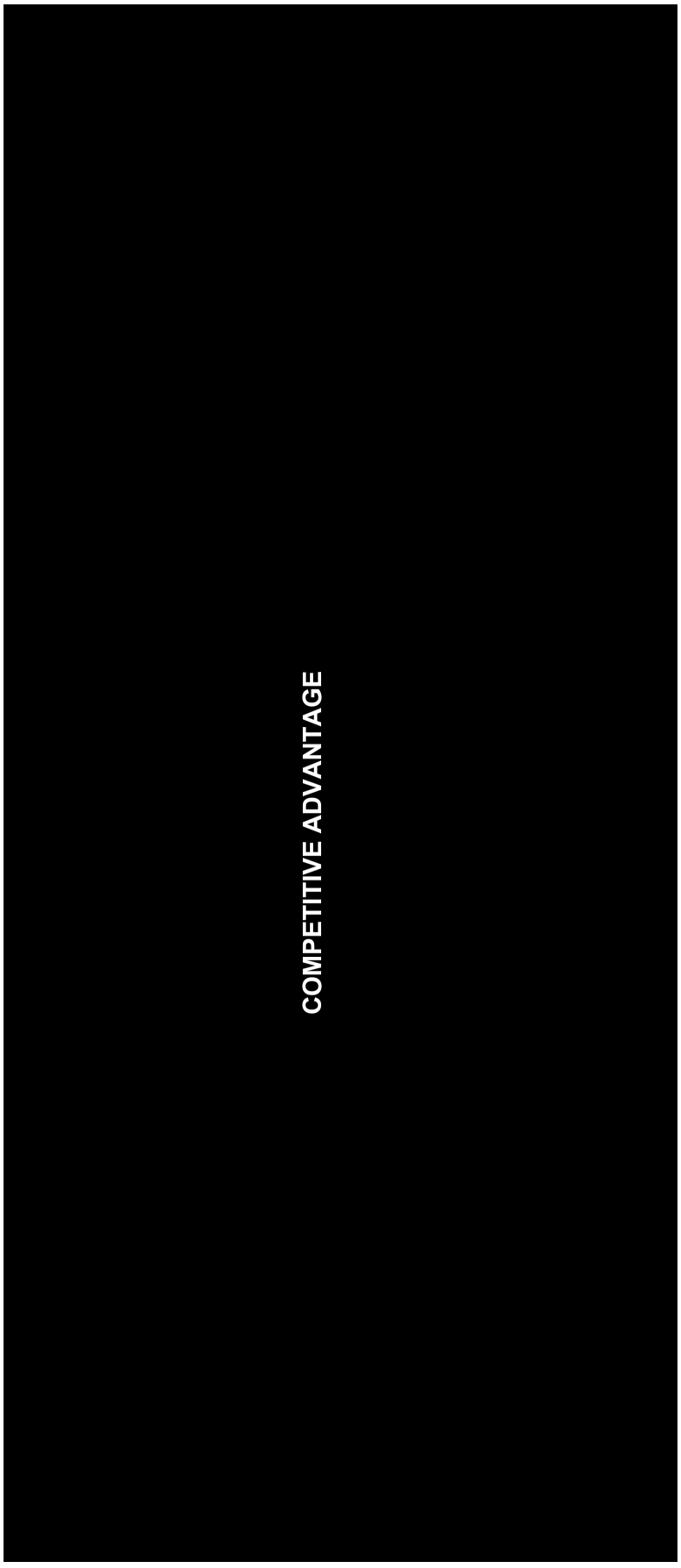

[e4]

Figure 3B-25 PSD of Typical Large Chug (025P)

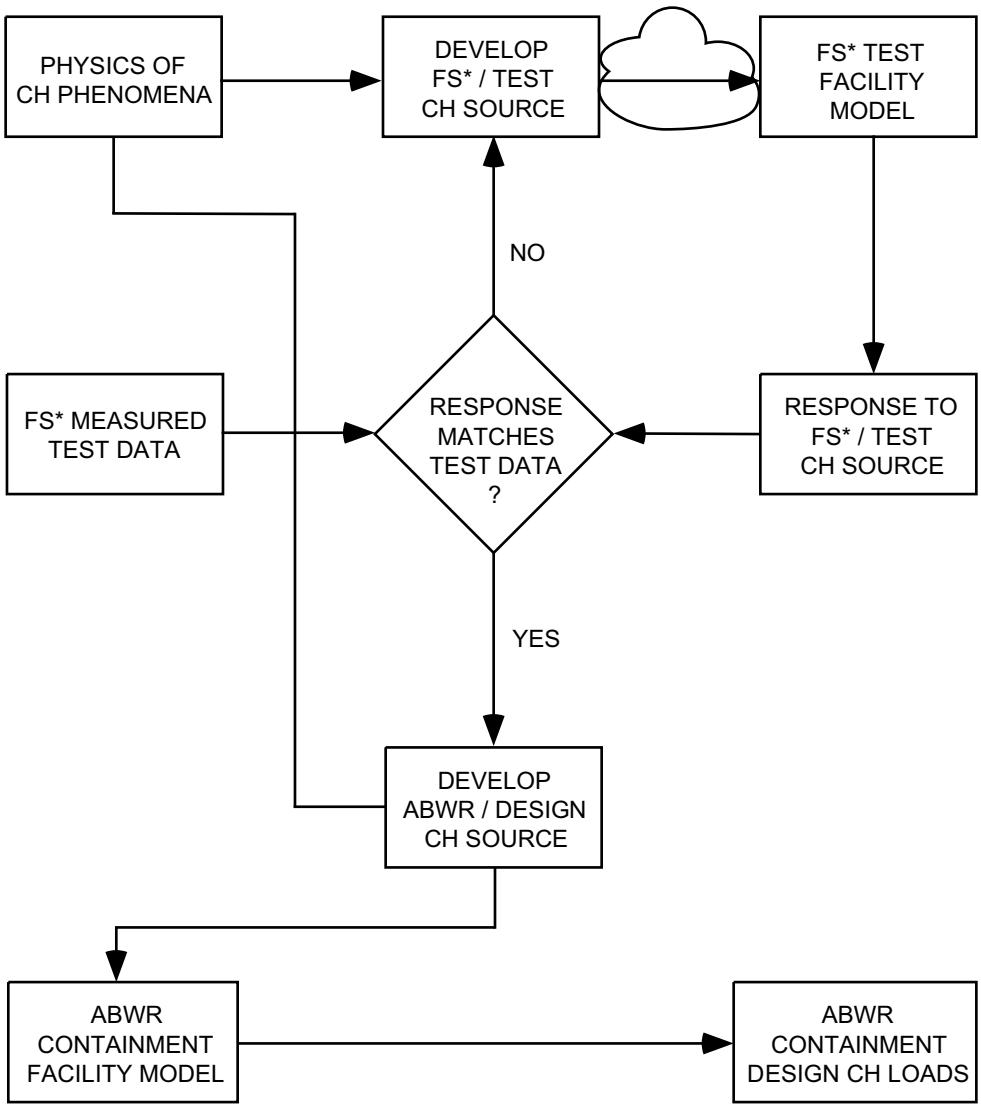

Figure 3B-26 ABWR Chug Source Load Methodology

[s4]

Figure 3B-27 Comparison of PSDs Between Analysis and Test

[e4]

[se]

COMPETITIVE ADVANTAGE

Figure 3B-29 Typical Wall Pressure Time History Due to CH

[e4]

[s4]

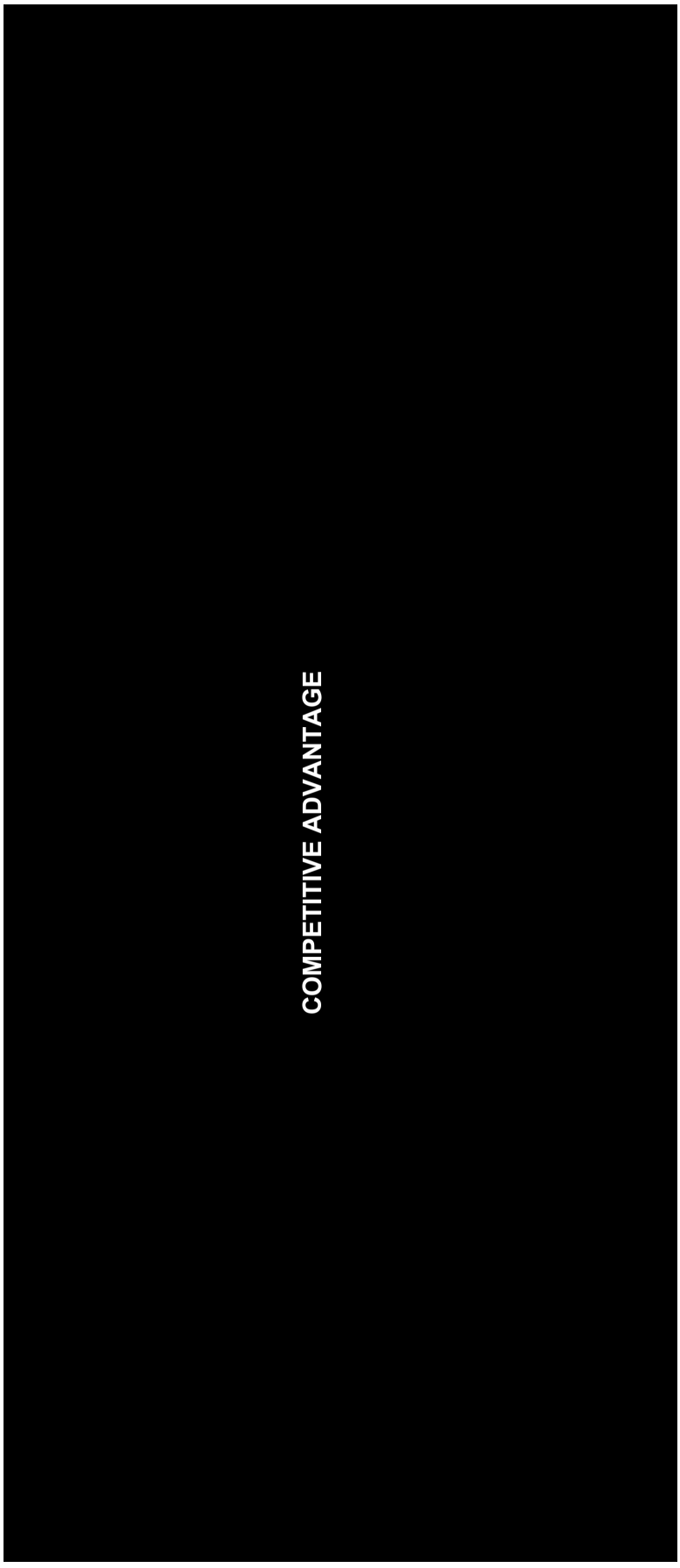

[e4]

Figure 3B-31 Typical Test Result of Upward Load on Horizontal Vent Due to CH

[se]

COMPETITIVE ADVANTAGE

Figure 3B-32 Typical Test Result of Moment Due on Horizontal Vent to CH

[e4]

[s4]

Figure 3B-33 Horizontal Vent Upward Loading for Vent Pipe and Pedestal

[e4]

[s4]

Figure 3B-34 Horizontal Vent Upward Loading for Structure Response Analysis

[e4]